

1
2 **Non-invasive Characterisation of Molecular Diffusion of Agent into Turbid**
3 **Matrix using Micro-SORS**
4
5
6

7 A. Botteon^{a,c*}, J. Yiming^b, S. Prati^b, G. Sciutto^b, M. Realini^a, C. Colombo^a, C. Castiglioni^c, P. Matousek^d, C.
8
9 Conti^{a*}
10

11
12
13
14
15 ^a *Consiglio Nazionale delle Ricerche, Istituto di Scienze del Patrimonio Culturale (ISPC), Via Cozzi 53, 20125,*
16
17 *Milano, Italy.*

18
19 ^b *Microchemistry and Microscopy Art Diagnostic Laboratory (M2ADL), University of Bologna - Ravenna*
20
21 *Campus, via Guaccimanni 42, 48100, Ravenna, Italy.*

22
23
24 ^c *Politecnico di Milano, Department of Chemistry, Materials and Chemical Engineering “G. Natta”, piazza*
25
26 *Leonardo da Vinci 32, 20131 Milano, Italy.*

27
28
29 ^d *Central Laser Facility, Research Complex at Harwell, STFC Rutherford Appleton Laboratory, UKRI, Harwell*
30
31 *Oxford, OX11 0QX, United Kingdom.*

32
33
34
35
36 * Corresponding authors: alessandra.botteon@polimi.it, claudia.conti@cnr.it
37
38

39
40 Key words: Micro-spatially offset Raman spectroscopy, diffusion, non-invasive, Cultural Heritage
41
42
43
44
45

46 **Abstract**
47

48 This study proposes a non-invasive analytical method to study the molecular diffusion of a chemical agent
49
50 into a turbid matrix with an emerging analytical technique, micro-Spatially Offset Raman Spectroscopy
51
52 (micro-SORS). Here, the micro-SORS concept has been extended from the analysis of chemically distinct
53
54 stratified layers to the studies and monitoring of the absorption and diffusion processes, addressing a key
55
56 analytical need in a number of areas including polymer, pharmaceutical, forensic and biomedical sciences.
57
58
59
60
61
62
63
64
65

1
2
3
4
5
6
7
8
9
10
11
12
13
14
15
16
17
18
19
20
21
22
23
24
25
26
27
28
29
30
31
32
33
34
35
36
37
38
39
40
41
42
43
44
45
46
47
48
49
50
51
52
53
54
55
56
57
58
59
60
61
62
63
64
65

In Cultural Heritage the knowledge of the penetration depth of a polymer used to consolidate or to protect an object or the absorption depth of solvents used during a cleaning procedure is crucial for the performance evaluation of restoration methods and their safety towards the work of art. To date the most common protocol for obtaining this type of information comprises the application of stratigraphical analysis on cross-sections prepared after taking a small amount of sample from the work of art. This approach is destructive and may lack of statistical meaning, since the analytical information is limited to the micro area of sampling. To overcome these drawbacks, in this study, micro-SORS was successfully used, for the first time, to non-invasively characterise the penetration of a polymer and of a viscous solvent into a gypsum substrate, permitting the reconstruction of the diffusion trends of the products into the matrix and the evaluation of their performances.

Introduction

The study of the diffusion of an agent into a turbid matrix is a fundamental topic in material science since the concentration profile and the penetration depth of the agent severely affect the final properties of the system. Plastics, papers, concretes and biological tissues can be affected by absorption or alteration processes with the consequent formation of concentration profiles, which have to be characterized for the in depth understanding of their performance. In Cultural Heritage field, the knowledge of the depth distribution of a product applied on the historical buildings or art objects surfaces for conservation purposes is crucial for assessing the efficacy of consolidation and protection treatments [1]; another important issue concerns the correct assessment of solvent diffusion and retention inside paint layers, for example, in evaluating new cleaning procedures. In fact, it is widely known that the use of not confined solvents for the cleaning of paintings may produce negative effects such as swelling, softening and thus affecting the optical and mechanical properties of the paint layers [2]. Finally the diffusion of the decay products, as the soluble salts, within the substrates (stone, plaster, stucco, etc.), brings essential

1 information on the extent of the decay processes required, for instance, for planning more suitable
2 restoration works [3].
3
4

5 To date, the main analytical techniques used in Cultural Heritage field for investigating the diffusion of
6 chemical agents and decay products in the substrates include scanning electron microscopy coupled with
7 energy dispersive spectrometry (SEM-EDS) [1][3], Fourier-transform infrared spectroscopy (FTIR) [4][5] and
8 Raman spectroscopy [1][6]. These are currently destructive in nature due to their need of resorting to cross
9 sectional analysis. Recently, alternative non-destructive techniques such as neutron imaging [7], X-ray
10 micro-computed tomography [8] or synchrotron diffraction imaging have been proposed for the same
11 purpose; however, these are not easily accessible tools and the direct retrieval of molecular composition of
12 organic, inorganic, crystalline and amorphous compounds, which is extremely important for their
13 unequivocal identification, is not fully accomplished by these techniques.
14
15
16
17
18
19
20
21
22
23
24
25
26

27 The novel aspect of the present study is the development of a new non-invasive analytical method to study,
28 at the molecular level, the diffusion of a chemical agent into a turbid matrix, using micro-Spatially Offset
29 Raman Spectroscopy (micro-SORS) [9][10], an emerging, accessible and relatively easily deployable
30 technique.
31
32
33
34
35
36
37

38 Micro-SORS is a conceptual evolution of its parent technique, (macro-scale) SORS [11][12], combining SORS
39 with microscopy. This enables to non-invasively resolve thin, micrometre scale layers such as painted
40 stratigraphy in the Cultural Heritage field or turbid stratified systems in polymer, catalytic, biological and
41 biomedical sciences. Micro-SORS represents an important tool in situations where a non-destructive and/or
42 non-invasive molecular analysis is required, e.g. when dealing with precious, unique samples or objects in
43 art field and forensic science.
44
45
46
47
48
49
50
51
52

53 Micro-SORS principles and associated concepts have been discussed extensively in literature recently [13–
54 23].
55
56
57

58 To date micro-SORS has been used to discriminate between the composition of different layers in stratified
59 matrixes. Here for the first time micro-SORS has been optimized to monitor the diffusion of an agent into a
60
61
62
63
64
65

1 turbid matrix, where there is no defined separation of compounds into chemically distinct layers. This proof
2 of concept study demonstrates that defocusing, the most basic micro-SORS variant, is capable to non-
3
4 invasively distinguish different penetration depths of conservation products and solvents into a matrix,
5
6 through the monitoring of their diffusion profiles. Two situations have been reproduced using laboratory
7
8 mock-up samples which have a substrate made of gypsum (i.e. simulating a gypsum-based stucco matrix)
9
10 but different applied products, namely an organic conservation product (Paraloid B72 – PB72), and DES, a
11
12 deep eutectic solvent (Choline chloride-Urea 1:2). PB72 is an acrylic copolymer that, since the 1950, has
13
14 been extensively applied as fixative and protective especially on wood, ceramic, glass, stone monuments
15
16 and plasters [24–27]. Choline chloride-Urea 1:2 DES and its based gels are a new type of eco-friendly
17
18 products [28] that are currently under evaluation for the removal of proteinaceous coatings from art
19
20 objects.
21
22
23
24
25
26

27 **Materials and Methods**

28
29
30
31
32
33 In the experiments, a matrix made of gypsum blocks (5cm x 5cm x 2cm) was used for the application of the
34
35 two products.
36
37

38 The first product was Paraloid B72 (PB72), an ethyl-methacrylate and methyl-acrylate copolymer commonly
39
40 used ad fixative, having good ageing proprieties and chemical stability [25][26]. The solution of Paraloid B72
41
42 (5% in acetone) was applied with a brush on the gypsum blocks surface. Two samples S1 and S2 have been
43
44 treated with an increasing amount of PB72 to obtain a different penetration depth of the product.
45
46
47

48 The second product was a deep eutectic solvent (DES), an innovative and eco-friendly product, having
49
50 similar physical-chemical properties to common ionic liquids (ILs) and several advantages over traditional
51
52 ILs such as lower price, easy storage and easy preparation [29]. Moreover, its efficacy for the extraction of
53
54 proteins has been demonstrated [30], unlocking the possibility of using it as a solvent in new green gels for
55
56 the removal of proteinaceous coating from paintings. Nonetheless, DES is a non-volatile solvent and thus it
57
58
59
60
61
62
63
64
65

1 is retained in a (porous) material, possibly altering its physical-chemical and optical properties. It is
2 therefore extremely important to evaluate the extent of the diffusion of this product in an artwork.
3

4
5 DES solvent was synthesized by mixing a hydrogen bond acceptor (Choline chloride) with a hydrogen
6 bonding donor (Urea), at the mole ratio 1:2 in a round bottom flask. The mixture was stirred at 100 °C for 5
7 min until a homogeneous colorless liquid was obtained. A drop of DES was applied on the S3 gypsum
8 surface and its diffusion was studied with micro-SORS measurements.
9

10
11 A DES drop exceeded the quantity of solvent that could penetrate in a matrix during a cleaning procedure.
12 Such relatively great amount was applied to enhance the DES Raman signal and thus to enable a better
13 monitoring of its absorption process with micro-SORS. Further studies on a more realistic scenario are in
14 progress, mimicking the standard cleaning procedures.
15

16
17 The experiments were carried out using a Senterra dispersive Raman microscope (Bruker Optik GmbH)
18 equipped with a Peltier cooled charge coupled device (CCD) detector (1,024 × 256 pixels) and a 785 nm
19 excitation laser.
20

21
22 Defocusing micro-SORS measurements were carried out on the intact samples after their interaction with
23 the products. The spectra were collected using a laser power of 100 mW and an acquisition time ranging
24 from 100 to 300 s. The measurements were carried out at imaged and defocused positions moving the
25 objective (20x magnification) away from the sample in z direction (from 0 to 1000 μm of distance).
26

27
28 Three series of defocusing micro-SORS measurements were acquired on the samples S1 and S2. As for S3,
29 the diffusion of DES was studied by performing a series of three micro-SORS acquisitions at t_0 (immediately
30 after the application of the drop) and three additional series at t_1 (after 20 h) to evaluate the behavior of
31 such an oleous compound over time.
32

33
34 The progressive decrease of the product signals with respect to gypsum was evaluated calculating the
35 intensity ratio between two selected Raman bands of the compounds. The decreasing trends observed for
36 the three series of each sample are reproducible; slight differences observed among them have to be
37
38
39
40
41
42
43
44
45
46
47
48
49
50
51
52
53
54
55
56
57
58
59
60
61
62
63
64
65

1 ascribed to the heterogeneity of the samples. To provide an easy data visualization, the intensity values
2 obtained for the three series were averaged to get a representative trend for each sample (the single series
3 are reported in the supplementary material).
4
5

6
7 Moreover, the cross-sections of S1 and S2 were prepared cutting and polishing a fragment of the samples.
8

9
10 The cross-sections were conventionally analysed with vertical linear scans to check the penetration depth
11 of PB72 and the outcomes were compared with the results obtained with defocusing micro-SORS. The
12 spectra were acquired using a 20x magnification objective, a laser power of 100 mW at the sample and an
13 acquisition time of 100 s per spectrum. Three line scans were performed, starting from the surface and
14 progressively moving to the internal part of the samples, with a step size of 50-100 μm . For each depths,
15 the PB72/Gypsum intensity ratio was calculated and averaged for the three line scans (in the
16 supplementary material, the single lines scans can be visualized).
17
18
19
20
21
22
23
24
25
26

27 The S3 actual penetration depth was not checked with cross-sectioned samples, since DES remains in a
28 liquid state in gypsum matrix, and can therefore move from its original position during the sample cutting
29 and polishing.
30
31
32
33
34

35 Calculations and plot construction were carried out using OPUS and ORIGIN softwares.
36
37
38
39

40 **Results and Discussion**

41 **Paraloid B72 on gypsum (S1 and S2)**

42
43
44
45 The penetration depth of PB72 was non-invasively studied with defocusing micro-SORS directly on the
46 mock up surface. To validate the method, conventional destructive Raman analyses were performed on the
47 cross-sectioned samples. The normalised micro-SORS Raman spectra acquired on S1 and S2 surfaces at
48 imaged position (which correspond to a conventional Raman spectrum) show the presence of both gypsum
49 and PB72 (Figure 1). Gypsum characteristic bands are visible at 1135, 1008, 670, 620, 495 and 415 cm^{-1} .
50
51
52
53
54
55
56
57
58
59
60
61
62
63
64
65

1 PB72 bands, located at 1725, 1450, 864 and 835 cm^{-1} are much less intense compared with the gypsum, and
2 this is consistent with the relatively low amount of PB72 in the samples.
3

4 As expected in S2, the PB72 Raman bands intensity is higher than in S1 because more product was applied
5 on the surface.
6

7
8
9 In the defocusing series, a progressive decrease of PB72 bands is observed in both S1 and S2 relative to
10 those of gypsum. In Figure 2, a defocusing series collected on S2 sample is reported to illustrate this trend.
11 The PB72/gypsum ratios (intensity ratio of two representative bands, namely bands at 1450 and 415 cm^{-1}
12 for PB72 and gypsum, respectively) were calculated, normalized and plotted against the defocusing
13 distance to highlight the trends obtained with the two samples. The ratio plot in Figure 3 shows the average
14 of three series collected on S1 and S2. In the supplementary material, the plots of the three single series of
15 S1 and S2 are reported (Figure S1 and Figure S2).
16
17
18
19
20
21
22
23
24

25 The two bands chosen for ratio calculation are the 1450 cm^{-1} band of PB72 (the most intense of the
26 compound, assigned to one of the C-H bending modes [31]) and the 415 cm^{-1} band of gypsum (SO_4
27 symmetric bending [32]). The latter was selected for its intensity as it is the most comparable to the one of
28 PB72 ensuring easier monitoring of the relative intensity changes with micro-SORS defocusing distances.
29
30
31
32
33
34
35
36
37
38
39
40
41
42
43
44
45
46
47
48
49
50
51
52
53
54
55
56
57
58
59
60
61
62
63
64
65

There is a distinct difference in the decay rates for S1 and S2 samples signals plotted as normalised intensity ratios: S1 shows a faster ratio decay. The faster drop in the ratio decay rate is attributed to the more rapid lowering of the product concentration with depth. Therefore, the different decay rates can be related to the different penetration depth of the product in the two samples. In this case, the faster ratio decay rate in S1 suggests a more superficial penetration of PB72.

With the conventional measurements on cross-section, PB72 Raman signal was detected up to 250 μm of depth in S1 and up to 500 μm of depth in S2. In the averaged plot shown in Figure 4 (see supplementary material, Figure S3 and Figure S4, for the single series), the normalized decrease of the PB72/Gypsum ratio with respect to the depth can be visualized. Therefore, defocusing and conventional measurements on cross-sections give consistent results, as with both methods the two samples show different ratio decay

1 rates: the ratio values obtained on the cross-section drop to zero more rapidly in S1 than in S2, as was
2 observed in the defocusing measurements.
3

4
5 In S2 cross-section, anomalous constant intensities ratio values are observed between 25 μm and 100 μm
6 (Figure 4), providing interesting information on the diffusion of the product which is probably affected by
7 the heterogeneous porosity of the matrix. Nonetheless, in line with expectations, this trend does not
8 emerge in the defocusing plot (Figure 3), because in defocusing measurements, enlarging the laser spot and
9 collection zones, the Raman signal is collected from a volume larger than the conventional measurements.
10 Therefore, defocusing intrinsically averages the Raman signal and some heterogeneities under the surface
11 can be missed.
12
13
14
15
16
17
18
19
20
21

22 **DES on gypsum (S3)**

23 In this sample, the micro-SORS measurements aim at monitoring the diffusion of DES into gypsum matrix in
24 time resolved manner. Therefore, two sets of defocusing micro-SORS measurements were performed. The
25 first set was performed immediately after DES application on sample surface (t_0). Afterwards, a series of
26 conventional spectra were repeated on the sample surface: a progressive lowering of DES bands was
27 registered, suggesting that DES was diffusing into the gypsum matrix. In the range between 20 and 30
28 hours after the application DES band intensity was constant, implying the end of the absorption process.
29 The second set of measurements was then performed at 30 hours (t_1).
30
31
32
33
34
35
36
37
38
39
40

41 Two imaged spectra collected at t_0 and t_1 are shown in Figure 5. The spectra are dominated by gypsum
42 Raman bands, but some of the bands ascribable to DES are also visible: the band at 716 cm^{-1} assigned to
43 the C-N symmetric stretching of choline and the C-N asymmetric stretching band of urea located at 1450
44 cm^{-1} [33]. At t_1 , the imaged spectrum shows less intense DES Raman bands because DES has leached away
45 from the surface. Upon performing micro-SORS experiments, it became evident that DES bands intensities
46 progressively decreased compared with gypsum ones as is illustrated in Figure 6.
47
48
49
50
51
52
53
54
55
56

57 For this sample, the 716 cm^{-1} band of DES and the 670 cm^{-1} Raman band of gypsum (SO_4 asymmetric
58 bending [32]) were used for the calculation of the solvent-substrate ratio. These Raman bands were
59 selected because of their intensities being comparable. The averaged ratio plots are shown in Figure 7,
60
61
62
63
64
65

1
2
3
4
5
6
7
8
9
10
11
12
13
14
15
16
17
18
19
20
21
22
23
24
25
26
27
28
29
30
31
32
33
34
35
36
37
38
39
40
41
42
43
44
45
46
47
48
49
50
51
52
53
54
55
56
57
58
59
60
61
62
63
64
65

whereas the ratio plots relative to the single series collected at t_0 and t_1 are reported in the supplementary material, Figure S5 and Figure S6. The normalized Raman intensity ratio plots obtained at t_0 and t_1 show different decay rates, as expected (Figure 7a): it is possible to observe that at t_1 the decrease of DES signals is less pronounced than at t_0 . The rapid decrease of the ratio values at t_0 is associated to a higher concentration of the product close to the surface, whereas the more constant ratio values obtained at t_1 are related to the deeper diffusion of the product inside the matrix.

It is noted that the ratio values of t_1 show a certain degree of fluctuation. This is ascribed to the Raman peak intensity of DES at t_1 being very low resulting in very small ratio values (see the not normalized ratio plot in Figure 7b) and noisier outcome. For S3, a cross-sectioned samples could not be analysed since DES, which remains liquid, can easily move from its original position during the sample cutting and polishing, rendering ineffective the monitoring of its distribution.

Conclusions

This study demonstrates the possibility of non-invasively assessing the concentration profiles of a product within an absorbent matrix using micro-SORS. In micro-SORS experiments the samples with different penetration depths of a product could be differentiated based on the decay rates of their agent-matrix Raman intensity ratio. The study is particularly beneficial to the Cultural Heritage field, as a non-invasive characterization ensures avoiding damage to art materials. Using this method, a wide range of situations could be non-invasively studied, that include the penetration depth of a fixative agent or a consolidant in a stucco, a plaster or a stone, and monitoring of the absorption process of a liquid, such as a cleaning solvent, under the exposed surface.

The measurements were performed using the most basic variant of micro-SORS, namely defocusing micro-SORS. This variant has the advantage of being compatible with existing micro-Raman instruments and its implementation does not require any instrumental nor software modifications. This work is therefore important by pointing out the potential of this ready-to-use method for monitoring of absorption processes.

1 At this stage of the development, defocusing micro-SORS does not allow the determination of the absolute
2 depth penetration reached by a product, instead it establishes if a product is more or is less deeply
3 penetrated in a sample compared to another sample. Nonetheless, these results suggest the possibility of
4 estimating the absolute penetration depth of an agent into matrix after a calibration set is prepared and
5 quantitative calibration established. The key requirement is, however, that the calibration set is built up
6 having the same matrix and the same agent combination as that for the measured sample.
7
8
9
10
11
12
13
14

15 References

- 16
17
18 [1] P.M. Carmona-Quiroga, S. Martínez-Ramírez, S. Sánchez-Cortés, M. Oujja, M. Castillejo, M.T. Blanco-
19 Varela, Effectiveness of antigrffiti treatments in connection with penetration depth determined by
20 different techniques, *J. Cult. Herit.* 11 (2010) 297–303.
21 <https://doi.org/10.1016/j.culher.2009.09.006>.
- 22 [2] A. Phenix, K. Sutherland, The cleaning of paintings: effects of organic solvents on oil paint films,
23 *Stud. Conserv.* 46 (2001) 47–60. <https://doi.org/10.1179/sic.2001.46.supplement-1.47>.
- 24 [3] R. Přikryl, J. Přikrylová, M. Racek, Z. Weishauptová, K. Kreislová, Decay mechanism of indoor porous
25 opuka stone: a case study from the main altar located in the St. Vitus Cathedral, Prague (Czech
26 Republic), *Environ. Earth Sci.* 76 (2017). <https://doi.org/10.1007/s12665-017-6596-7>.
- 27 [4] F. Casadio, L. Toniolo, Polymer Treatments for Stone Conservation: Methods for Evaluating
28 Penetration Depth, *J. Am. Inst. Conserv.* 43 (2004) 3–21.
29 <https://doi.org/10.1179/019713604806112623>.
- 30 [5] G. Graziani, E. Sassoni, G.W. Scherer, E. Franzoni, Penetration depth and redistribution of an
31 aqueous ammonium phosphate solution used for porous limestone consolidation by brushing and
32 immersion, *Constr. Build. Mater.* 148 (2017) 571–578.
33 <https://doi.org/10.1016/j.conbuildmat.2017.05.097>.
- 34 [6] C. Conti, C. Colombo, D. Dellasega, M. Matteini, M. Realini, G. Zerbi, Ammonium oxalate treatment:
35 Evaluation by μ -Raman mapping of the penetration depth in different plasters, *J. Cult. Herit.* 12
36 (2011) 372–379. <https://doi.org/10.1016/j.culher.2011.03.004>.
- 37 [7] F. Hameed, B. Schillinger, A. Rohatsch, M. Zawisky, H. Rauch, Investigations of stone consolidants by
38 neutron imaging, *Nucl. Instruments Methods Phys. Res. Sect. A Accel. Spectrometers, Detect. Assoc.*
39 *Equip.* 605 (2009) 150–153. <https://doi.org/10.1016/j.nima.2009.01.139>.
- 40 [8] M. Slavíková, F. Krejčí, J. Žemlička, M. Pech, P. Kotlík, J. Jakůbek, X-ray radiography and tomography
41 for monitoring the penetration depth of consolidants in Opuka - the building stone of Prague
42 monuments, *J. Cult. Herit.* 13 (2012) 357–364. <https://doi.org/10.1016/j.culher.2012.01.010>.
- 43 [9] C. Conti, C. Colombo, M. Realini, G. Zerbi, P. Matousek, Subsurface Raman analysis of thin painted
44 layers, *Appl. Spectrosc.* 68 (2014) 686–691. <https://doi.org/10.1366/13-07376>.
- 45 [10] C. Conti, C. Colombo, M. Realini, P. Matousek, Subsurface analysis of painted sculptures and plasters
46 using micrometre-scale spatially offset Raman spectroscopy (micro-SORS), *J. Raman Spectrosc.* 46
47 (2015) 476–482. <https://doi.org/10.1002/jrs.4673>.
- 48 [11] P. Matousek, M.D. Morris, N. Everall, I.P. Clark, M. Towrie, E. Draper, A. Goodship, A.W. Parker,
49 Numerical simulations of subsurface probing in diffusely scattering media using spatially offset
50 Raman spectroscopy, *Appl. Spectrosc.* 59 (2005) 1485–1492.
51 <https://doi.org/10.1366/000370205775142548>.
- 52 [12] K. Buckley, P. Matousek, Non-invasive analysis of turbid samples using deep Raman spectroscopy,
53 *Analyst.* 136 (2011) 3039–3050. <https://doi.org/10.1039/c0an00723d>.
- 54 [13] C. Conti, M. Realini, C. Colombo, P. Matousek, Comparison of key modalities of micro-scale spatially
55
56
57
58
59
60
61
62
63
64
65

- offset Raman spectroscopy, *Analyst*. 140 (2015) 8127–8133. <https://doi.org/10.1039/c5an01900a>.
- [14] Z. Di, B.H. Hokr, H. Cai, K. Wang, V. V Yakovlev, A. V Sokolov, M.O. Scully, Spatially offset Raman microspectroscopy of highly scattering tissue: Theory and experiment, *J. Mod. Opt.* 62 (2015) 97–101. <https://doi.org/10.1080/09500340.2014.976598>.
- [15] M. Realini, C. Conti, A. Botteon, C. Colombo, P. Matousek, Development of a full micro-scale spatially offset Raman spectroscopy prototype as a portable analytical tool, *Analyst*. 142 (2017) 351–355. <https://doi.org/10.1039/c6an02470j>.
- [16] K. Buckley, C.G. Atkins, D. Chen, H.G. Schulze, D. V Devine, M.W. Blades, R.F.B. Turner, Non-invasive spectroscopy of transfusable red blood cells stored inside sealed plastic blood-bags, *Analyst*. 141 (2016) 1678–1685. <https://doi.org/10.1039/c5an02461g>.
- [17] M. Realini, A. Botteon, C. Conti, C. Colombo, P. Matousek, Development of portable defocusing micro-scale spatially offset Raman spectroscopy, *Analyst*. 141 (2016) 3012–3019. <https://doi.org/10.1039/c6an00413j>.
- [18] A. Botteon, C. Colombo, M. Realini, S. Bracci, D. Magrini, P. Matousek, C. Conti, Exploring street art paintings by microspatially offset Raman spectroscopy, *J. Raman Spectrosc.* 49 (2018) 1652–1659. <https://doi.org/10.1002/jrs.5445>.
- [19] A. Rousaki, A. Botteon, C. Colombo, C. Conti, P. Matousek, L. Moens, P. Vandenabeele, Development of defocusing micro-SORS mapping: A study of a 19th century porcelain card, *Anal. Methods*. 9 (2017) 6435–6442. <https://doi.org/10.1039/c7ay02336g>.
- [20] C. Conti, A. Botteon, C. Colombo, M. Realini, P. Matousek, Fluorescence suppression using micro-scale spatially offset Raman spectroscopy, *Analyst*. 141 (2016) 5374–5381. <https://doi.org/10.1039/c6an00852f>.
- [21] A. Botteon, C. Conti, M. Realini, C. Colombo, P. Matousek, Discovering Hidden Painted Images: Subsurface Imaging Using Microscale Spatially Offset Raman Spectroscopy, *Anal. Chem.* 89 (2017) 792–798. <https://doi.org/10.1021/acs.analchem.6b03548>.
- [22] C. Conti, A. Botteon, C. Colombo, M. Realini, P. Matousek, Investigation of Heterogeneous Painted Systems by Micro-Spatially Offset Raman Spectroscopy, *Anal. Chem.* 89 (2017) 11476–11483. <https://doi.org/10.1021/acs.analchem.7b02700>.
- [23] P. Vandenabeele, C. Conti, A. Rousaki, L. Moens, M. Realini, P. Matousek, Development of a Fiber-Optics Microspatially Offset Raman Spectroscopy Sensor for Probing Layered Materials, *Anal. Chem.* 89 (2017) 9218–9223. <https://doi.org/10.1021/acs.analchem.7b01978>.
- [24] G.M. Crisci, M.F. La Russa, M. Malagodi, S.A. Ruffolo, Consolidating properties of Regalrez 1126 and Paraloid B72 applied to wood, *J. Cult. Herit.* 11 (2010) 304–308. <https://doi.org/10.1016/j.culher.2009.12.001>.
- [25] M.F. Vaz, J. Pires, A.P. Carvalho, Effect of the impregnation treatment with Paraloid B-72 on the properties of old Portuguese ceramic tiles, *J. Cult. Herit.* 9 (2008) 269–276. <https://doi.org/10.1016/j.culher.2008.01.003>.
- [26] S. Chapman, D. Mason, Literature Review: The Use of Paraloid B-72 as a Surface Consolidant for Stained Glass, *J. Am. Inst. Conserv.* 42 (2003) 381–392. <https://doi.org/10.1179/019713603806112813>.
- [27] S. Bracci, M.J. Melo, Correlating natural ageing and Xenon irradiation of Paraloid® B72 applied on stone, *Polym. Degrad. Stab.* 80 (2003) 533–541. [https://doi.org/10.1016/S0141-3910\(03\)00037-5](https://doi.org/10.1016/S0141-3910(03)00037-5).
- [28] E.L. Smith, A.P. Abbott, K.S. Ryder, Deep Eutectic Solvents (DESs) and Their Applications, *Chem. Rev.* 114 (2014) 11060–11082. <https://doi.org/10.1021/cr300162p>.
- [29] C. Ruß, B. König, Low melting mixtures in organic synthesis – an alternative to ionic liquids?, *Green Chem.* 14 (2012) 2969–2982. <https://doi.org/10.1039/c0xx00000x>.
- [30] Q. Zeng, Y. Wang, Y. Huang, X. Ding, J. Chen, K. Xu, Deep eutectic solvents as novel extraction media for protein partitioning, *Analyst*. 139 (2014) 2565–2573. <https://doi.org/10.1039/c3an02235h>.
- [31] M.. DOMENECH-CARBO, A. DOMENECH-CARBO, J.. Gileno-Adelantado, B.-R. F., Identification of Synthetic Resins Used in Works of Art by, *Appl. Spectrosc.* 55 (2001).
- [32] N. Buzgar, A. Buzatu, I. Sanislav, The Raman study on certain sulfates, *Analele Stiint. Ale Univ. Al. I. Cuza.* 55 (2009) 5–23.
- [33] B. Bozzini, B. Busson, C. Humbert, C. Mele, A. Tadjeddine, Electrochemical fabrication of nanoporous

1 gold decorated with manganese oxide nanowires from eutectic urea/choline chloride ionic liquid.
2 Part III – Electrodeposition of Au–Mn: a study based on in situ Sum-Frequency Generation and
3 Raman spectroscopies, *Electrochim. Acta.* 218 (2016) 208–215.
4 <https://doi.org/10.1016/j.electacta.2016.09.077>.
5
6

7 **Figures Captions**

8
9
10 *Figure 1: Raman spectra (black) collected on S1 and S2 surfaces at imaged position (corresponding to*
11 *conventional Raman measurements), normalized to the most intense gypsum band at 1008 cm^{-1} . The*
12 *reference spectra of PB72 and gypsum are also reported (red).*
13
14

15
16
17
18
19 *Figure 2: Representative defocusing micro-SORS series collected on S2 sample and normalized to 415 cm^{-1}*
20 *band of gypsum. The micro-SORS defocusing steps are indicated (values typed in different colours). A*
21 *progressive relative decrease of PB72 Raman band intensity is observed with increasing defocusing distance.*
22
23

24
25
26
27
28
29 *Figure 3: PB72/Gypsum averaged and normalized ratios of S1 and S2. The two penetration depths can be*
30 *distinguished through the different intensities ratio decay rates of the samples.*
31
32

33
34
35
36 *Figure 4: PB72/Gypsum averaged and normalized ratio plot obtained for the conventional Raman spectra*
37 *performed on the cross-sectioned S1 and S2 samples: two different intensities ratio decay rates are*
38 *observed.*
39
40
41

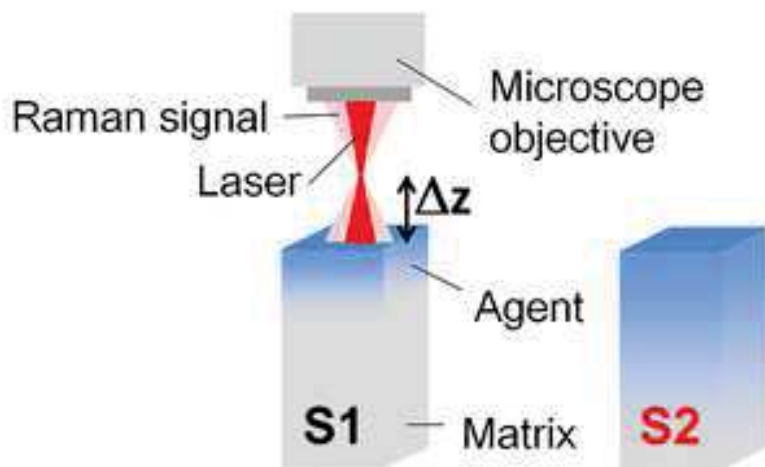
42
43
44
45 *Figure 5: Raman spectra obtained at imaged position on S3 surface at t_0 and t_1 (black) and reference spectra*
46 *of DES and gypsum (red).*
47
48

49
50
51
52
53 *Figure 6: Representative defocusing sequence of spectra acquired at t_0 on S3 and normalized to gypsum*
54 *band at 670 cm^{-1} . The micro-SORS steps are indicated (values typed in different colours). A progressive*
55 *relative decrease of DES Raman band intensity is observed by increasing the defocusing distance.*
56
57
58
59
60
61
62
63
64
65

Figure 7: (a) normalized and (b) not normalized DES/Gypsum averaged ratios of micro-SORS series of S3. The penetration depths at t_0 and t_1 are evidenced by different intensities ratio decay rates (a).

1
2
3
4
5
6
7
8
9
10
11
12
13
14
15
16
17
18
19
20
21
22
23
24
25
26
27
28
29
30
31
32
33
34
35
36
37
38
39
40
41
42
43
44
45
46
47
48
49
50
51
52
53
54
55
56
57
58
59
60
61
62
63
64
65

Micro-SORS measurements



Raman intensity ratio plot

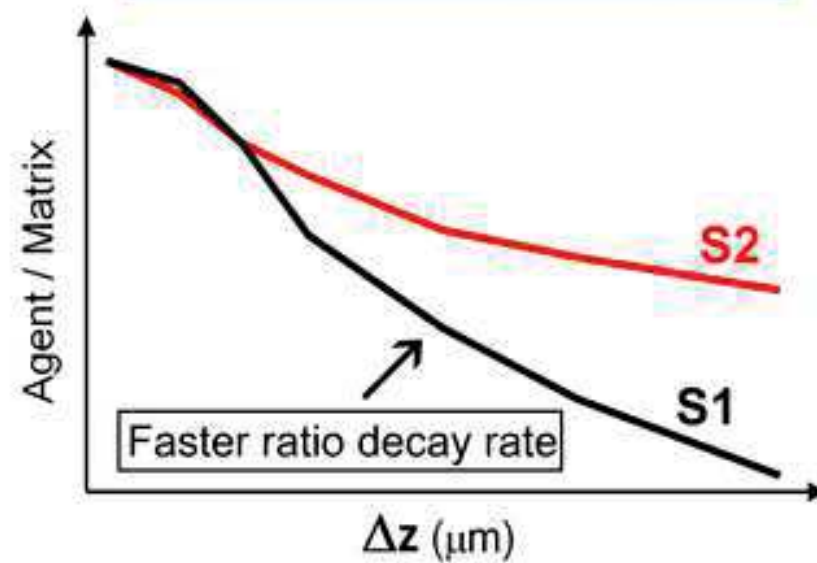


Figure 1 TIF
[Click here to download high resolution image](#)

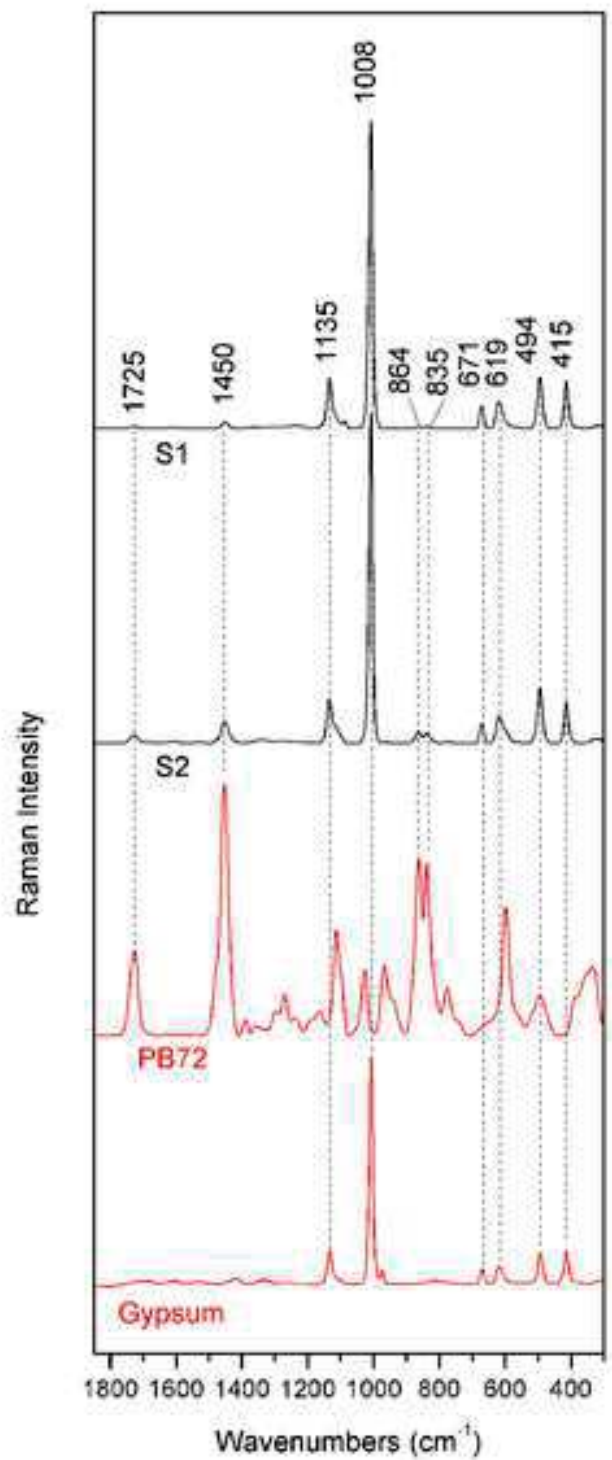


Figure 2 TIF

[Click here to download high resolution image](#)

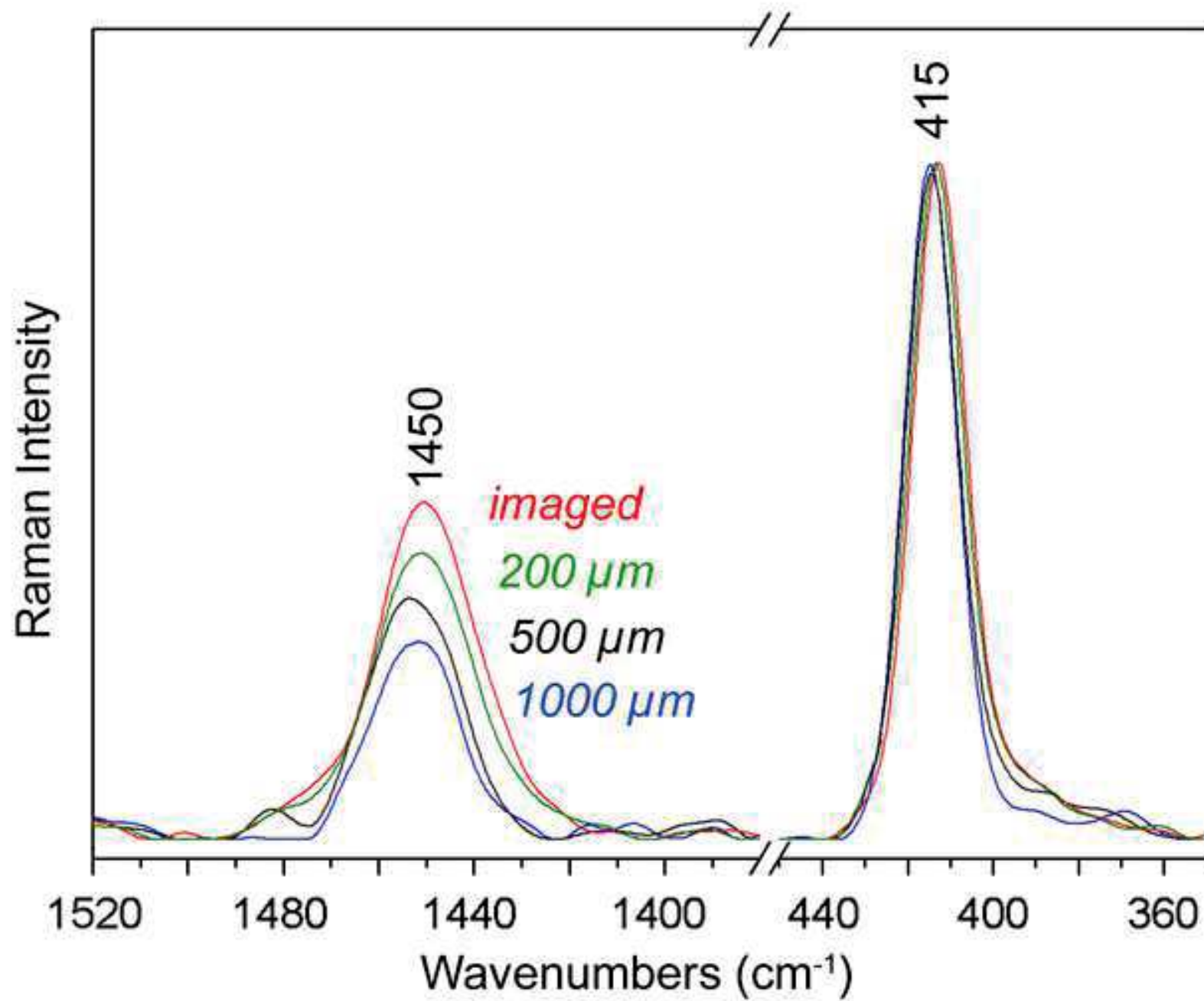


Figure 3 TIF

[Click here to download high resolution image](#)

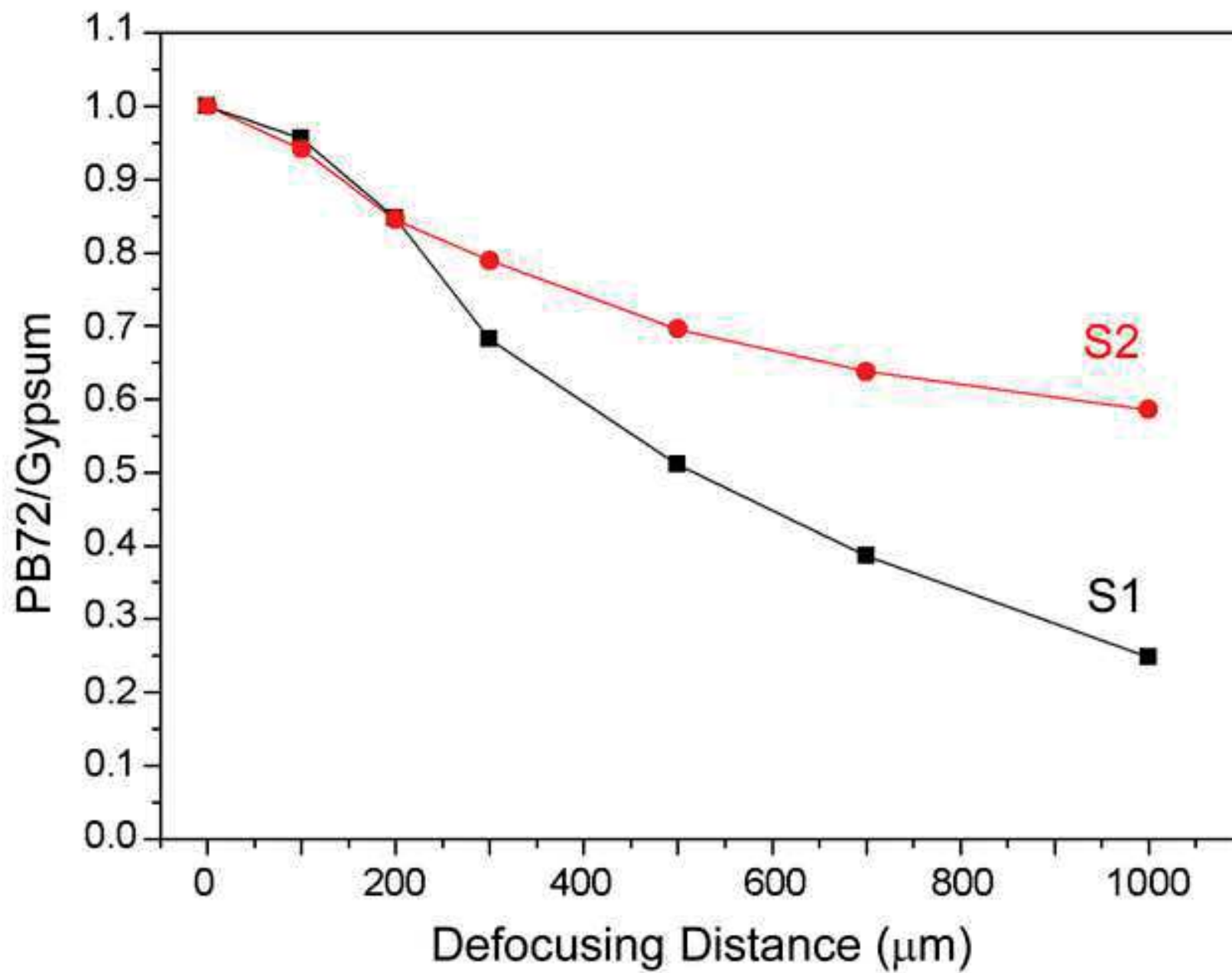


Figure 4 TIF

[Click here to download high resolution image](#)

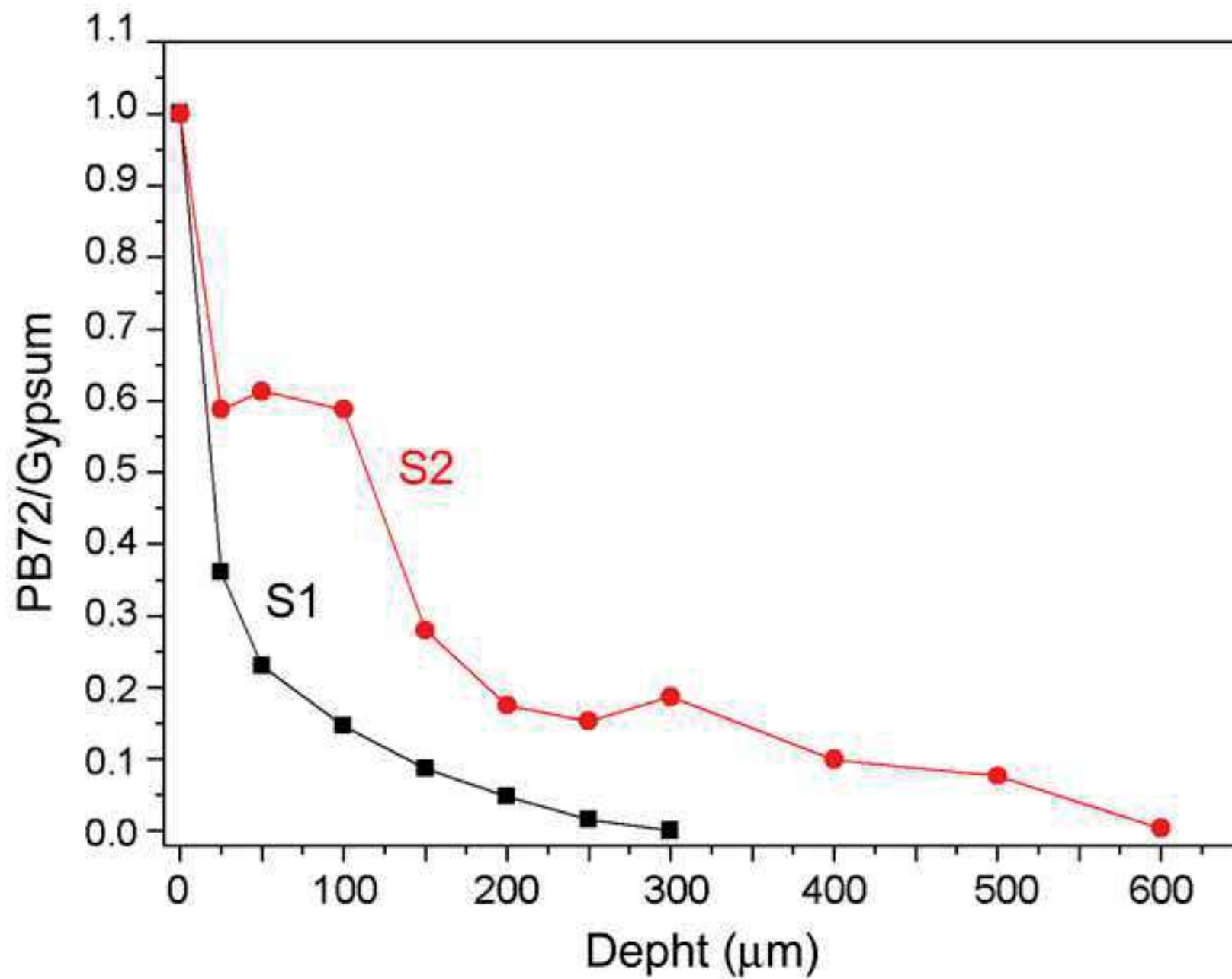


Figure 5 TIF
[Click here to download high resolution image](#)

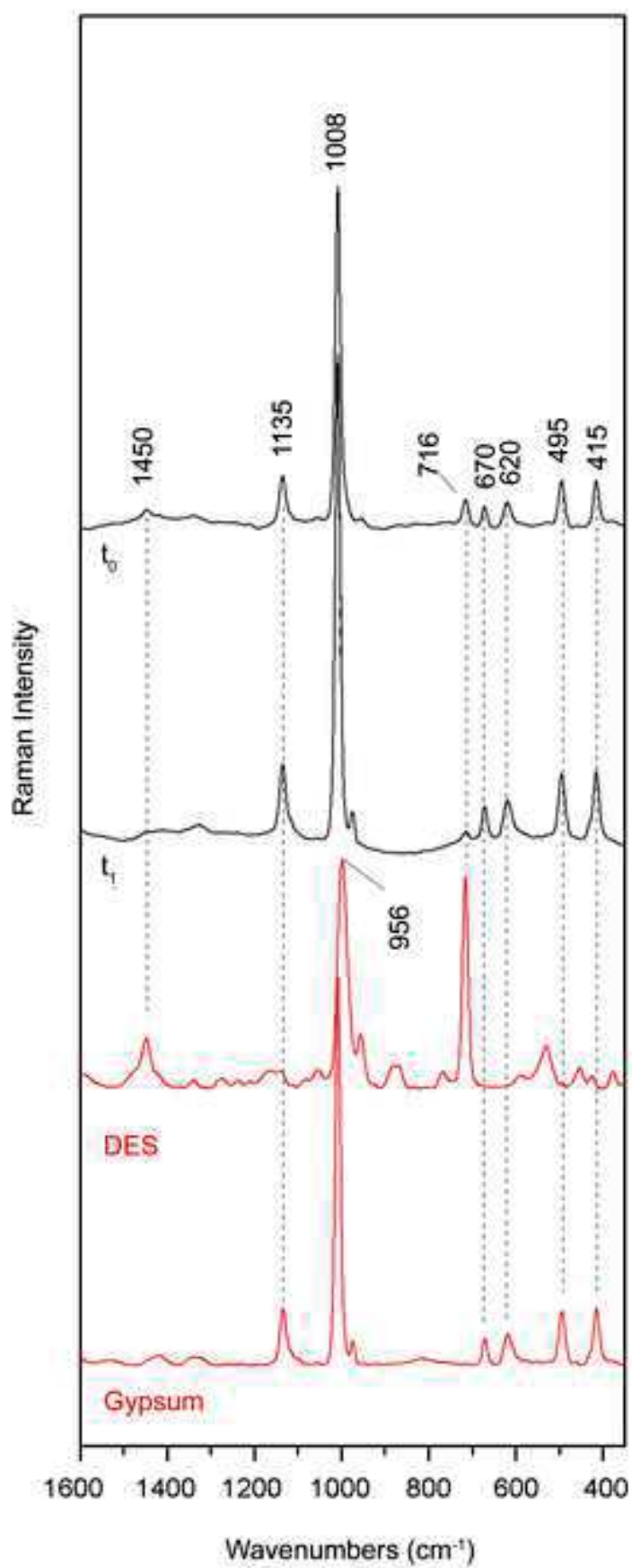


Figure 6 TIF

[Click here to download high resolution image](#)

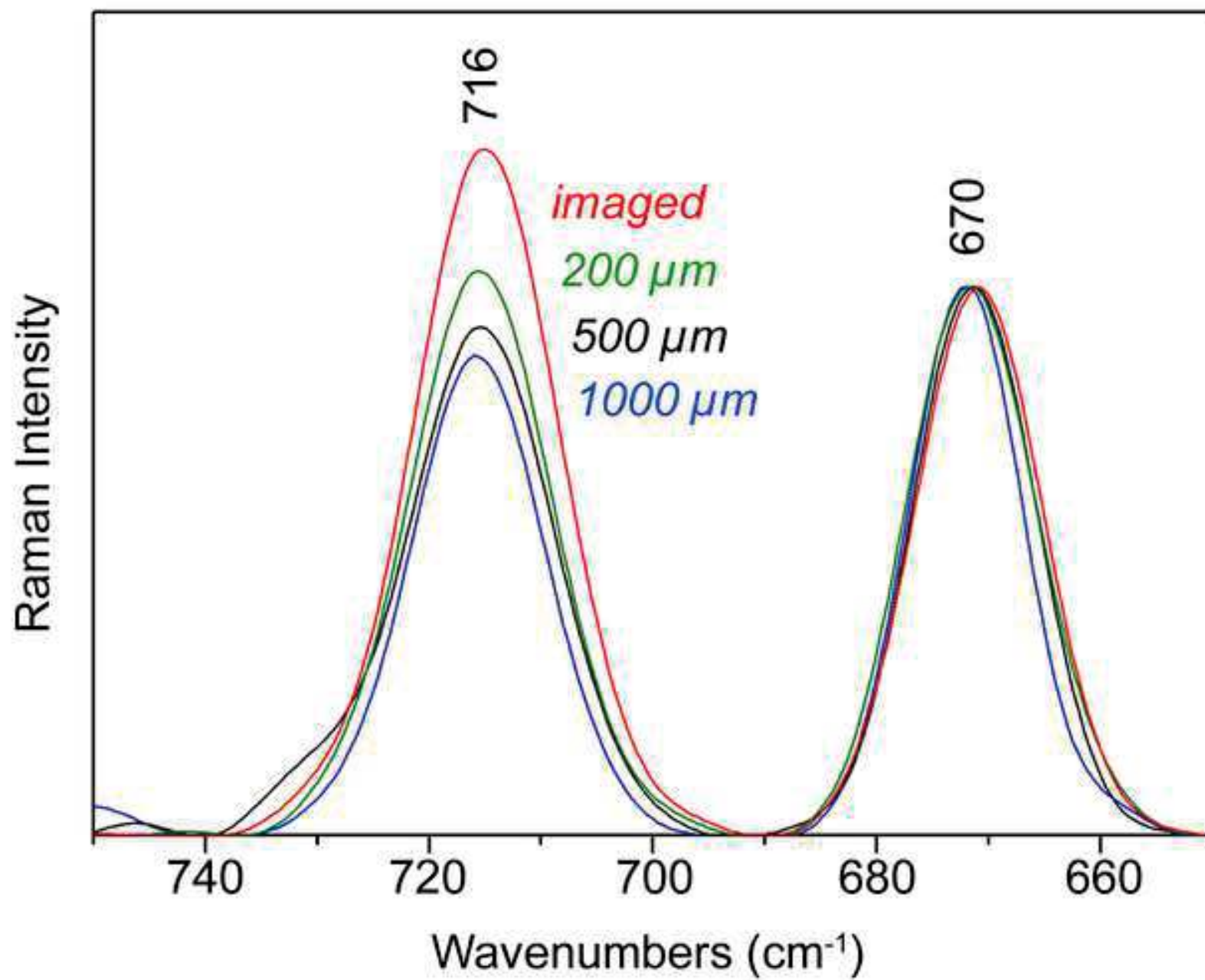
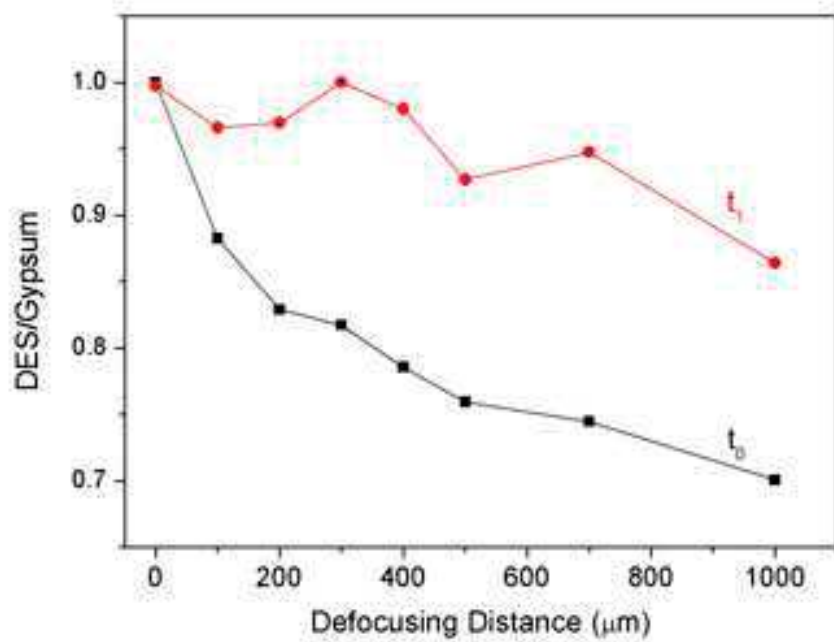
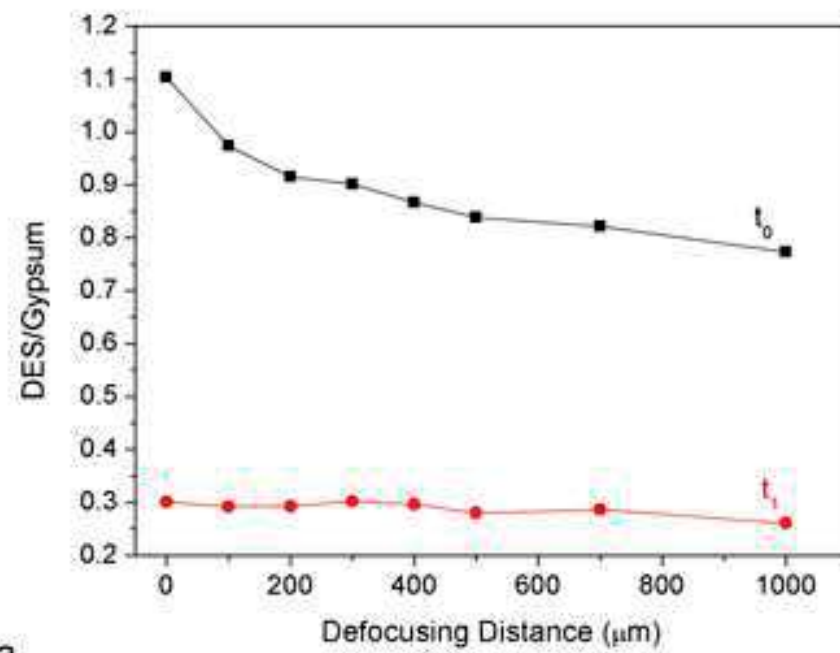


Figure 7 TIF

[Click here to download high resolution image](#)



a



b